

The Method of Fundamental Solutions for Solving Exterior Axisymmetric Helmholtz Problems with High Wave-Number

Wen Chen^{1,*}, Ji Lin¹ and C. S. Chen²

¹ College of Engineering Mechanics, Hohai University, Nanjing 210098, Jiangsu, China

² Department of Mathematics, University of Southern Mississippi, Hattiesburg, MS 39406, USA

Received 5 July 2012; Accepted (in revised version) 8 September 2012

Available online 7 June 2013

Dedicated to Graeme Fairweather on the occasion of his 70th birthday.

Abstract. In this paper, we investigate the method of fundamental solutions (MFS) for solving exterior Helmholtz problems with high wave-number in axisymmetric domains. Since the coefficient matrix in the linear system resulting from the MFS approximation has a block circulant structure, it can be solved by the matrix decomposition algorithm and fast Fourier transform for the fast computation of large-scale problems and meanwhile saving computer memory space. Several numerical examples are provided to demonstrate its applicability and efficacy in two and three dimensional domains.

AMS subject classifications: 65M10, 78A48

Key words: Method of fundamental solutions, exterior Helmholtz problem, circulant matrix, fast Fourier transform, axisymmetric domain.

1 Introduction

The method of fundamental solutions (MFS) [4, 11, 13, 14, 23], known for its simplicity and accuracy, has been gaining in popularity in various areas of scientific computing. Like the boundary element method (BEM) [3], it is applicable when the fundamental solution of the governing equation is known in advance. Numerical solution of the MFS is approximated by a linear combination of the fundamental solutions in terms of singularities which are placed outside the domain of the problem under consideration. The singularities of fundamental solutions can be either free or fixed which will result in, respectively, a nonlinear least square problem or a linear system [11]. A review of some

*Corresponding author.

Email: chenwen@hhu.edu.cn (W. Chen)

related work as well as varieties of applications and advantages over other methods can be found in [12, 14, 16, 25, 27, 32].

It is known that the MFS is particularly efficient and accurate for solving exterior Helmholtz problems since it is a truly boundary-type meshless method and the fundamental solution of the governing equations naturally satisfies the Sommerfeld radiation condition [2, 12, 14]. On the other hand, it is also known that the coefficient matrix generated by the MFS is often dense and ill-conditioned [6, 8, 33]. Direct solver for such a matrix requires $\mathcal{O}(N^3)$ operations and $\mathcal{O}(N^2)$ storages. As a result, the MFS is not feasible for solving exterior Helmholtz problems with high wave-number since massive collocation points are required. Furthermore, when the number of collocation points is large, the coefficient matrix becomes extremely ill-conditioned [7, 26]. In the past, the domain decomposition method (DDM), regularization techniques etc. [1, 24, 34] have been proposed to alleviate the conditioning and storage problems associated with the MFS formulation. In general, it is known that the structure of the coefficient matrix is closely related to the distribution of collocation points. If the collocation points and the solution domain are chosen in a particular fashion, the resulting matrix system has a certain structure. Recently, efficient algorithms have been developed for solving axisymmetric homogeneous differential equations in context of the MFS [10, 17–21, 28, 29, 31].

In this paper, our main goal is to develop an efficient numerical algorithm to solve high wave-number exterior Helmholtz problems in axisymmetric domain which has not been reported in literatures. The main problems rest on the high wave-number and Neumann boundary condition, for the fact that massive collocation points should be used to high wave-number problems and Neumann boundary condition may result in some structural damage to the coefficient matrix. By the radial properties of the fundamental solution and radial symmetric of the solution domain, we show the circulant or block circulant features of the coefficient matrices for problems under pure Dirichlet or Neumann boundary condition. And we take advantage of the special features of the circulant matrix [9] to accelerate the solution procedure. The key idea behind this algorithm is the matrix decomposition algorithm which has been widely circulated in science and engineering. For more details, we refer readers to the References [18–20]. Overall, the proposed algorithm decomposes the give system of equations into a series of linear systems of lower rank. Similar to the traditional matrix decomposition method, the proposed algorithm makes extensive use of fast Fourier transform which results in additional saving in the computational time and memory storage.

The rest of the paper is organized as follows. In Section 2, we give a general formulation of the MFS to exterior Helmholtz problems. In Section 3, through the use of the circulant matrix and fast Fourier transform, we describe how the matrix decomposition method is being used for solving both two and three dimensional problems. The efficacy of the proposed technique for solving Helmholtz problems with high wave-number is demonstrated by several benchmark examples in Section 4. In Section 5, we conclude with some discussion for the direction of future research.

2 The method of fundamental solutions

Let $\Omega \subset \mathbb{R}^d$, $d = 2, 3$, be a bounded domain. The region Ω_+ represents the unbounded domain exterior to Ω with a closed boundary Γ . In this paper we consider the following exterior Helmholtz problem

$$\nabla^2 u(\mathbf{x}) + k^2 u(\mathbf{x}) = 0, \quad \mathbf{x} \in \Omega_+, \tag{2.1}$$

where ∇^2 is the Laplacian, k the wave-number, with the Dirichlet or Neumann boundary condition

$$u(\mathbf{x}) = f(\mathbf{x}) \quad \text{or} \quad \frac{\partial u(\mathbf{x})}{\partial n} = f(\mathbf{x}), \quad \mathbf{x} \in \Gamma. \tag{2.2}$$

In order to obtain a unique solution to (2.1)-(2.2), the solution u must satisfy the Sommerfeld radiation condition at infinity [5, 35]

$$\lim_{r \rightarrow \infty} r^{\frac{d-1}{2}} \left(\frac{\partial}{\partial r} - ik \right) u(r) = 0, \tag{2.3}$$

where d denotes the dimension of the exterior problem, and $i = \sqrt{-1}$.

In the MFS, the approximate solution of the given differential equation is expressed as a linear combination of fundamental solution of the governing equation (2.1)

$$u(\mathbf{x}_i) = \sum_{j=1}^N \beta_j u_n^*(\mathbf{x}_i - \mathbf{y}_j), \quad \mathbf{x}_i \in \Gamma \cup \Omega_+, \tag{2.4}$$

where $\{\beta_j\}$ is the unknown coefficients, N the number of source points \mathbf{y}_j , and u_n^* is the fundamental solution of Helmholtz operator given by

$$\begin{cases} u_n^*(\mathbf{x}_i - \mathbf{y}_j) = \frac{i}{4} H_0^1(k \|\mathbf{x}_i - \mathbf{y}_j\|), & \mathbf{x}_i, \mathbf{y}_j \in \mathbb{R}^2, \\ u_n^*(\mathbf{x}_i - \mathbf{y}_j) = \frac{e^{ik \|\mathbf{x}_i - \mathbf{y}_j\|}}{\|\mathbf{x}_i - \mathbf{y}_j\|}, & \mathbf{x}_i, \mathbf{y}_j \in \mathbb{R}^3, \end{cases} \tag{2.5}$$

where $\|\cdot\|$ denotes the Euclidean norm, H_0^1 the Hankel function of the first kind of order zero. To avoid the singularity in the MFS formulation, we place the source points $\{\mathbf{y}_j\}$ on the fictitious boundary $\bar{\Omega}$ located inside Ω . Collocating boundary condition (2.2) and the Sommerfeld radiation condition (2.3) at all the collocation points, we have

$$\sum_{j=1}^N \beta_j u_n^*(\mathbf{x}_i - \mathbf{y}_j) = f(\mathbf{x}_i), \quad i = 1, 2, \dots, N, \tag{2.6a}$$

or

$$\sum_{j=1}^N \beta_j \frac{\partial u_n^*(\mathbf{x}_i - \mathbf{y}_j)}{\partial n} = f(\mathbf{x}_i), \quad i = 1, 2, \dots, N. \tag{2.6b}$$

It is noted that the fundamental solutions (2.5) naturally satisfies the Sommerfeld radiation condition (2.3) at infinity. Finally, the resulting system of equations is obtained by (2.6), from which we can obtain the unknown variables $\{\beta_j\}$. If the solvability of the matrix equation (2.6) is an issue, we can always use least square method to obtain $\{\beta_j\}$. Hence, the approximate solution of (2.1)-(2.2) can be obtained by (2.4) with known coefficients $\{\beta_j\}$ at any points in the solution domain.

3 Circulant matrix and fast solution

In this paper, we consider special cases of the Helmholtz equation in the axisymmetric domains. We will also prove that if the collocation points on the physical boundary and source points on the fictitious boundary are chosen in a particular fashion, the resulting system has a certain structure which can be exploited for the efficient solution of the given system.

We first consider the two dimensional problem on the exterior of a circular disk with radius r , a set of collocation points $\{x_i\}_{i=1}^N$ is chosen on boundary Γ by the following way

$$x_i = (r \cos(\psi_i), r \sin(\psi_i)),$$

where

$$\psi_i = \frac{2(i-1)\pi}{N}, \quad i = 1, 2, \dots, N. \tag{3.1}$$

Similarly, the singularities $\{y_j\}_{j=1}^N$ are chosen on the concentric circle inside Ω , as follows

$$y_j = (r_y \cos(\psi_j), r_y \sin(\psi_j)),$$

where $r_y = sr$ and $0 < s < 1$. From (2.6), we have the following matrix equation

$$A\beta = f, \tag{3.2}$$

where

$$A = \begin{pmatrix} u_n^*(x_1 - y_1) & u_n^*(x_1 - y_2) & \cdots & u_n^*(x_1 - y_N) \\ u_n^*(x_2 - y_1) & u_n^*(x_2 - y_2) & \cdots & u_n^*(x_2 - y_N) \\ \vdots & \vdots & \ddots & \vdots \\ u_n^*(x_N - y_1) & u_n^*(x_N - y_2) & \cdots & u_n^*(x_N - y_N) \end{pmatrix} \tag{3.3}$$

or

$$A = \begin{pmatrix} \frac{\partial u_n^*(x_1 - y_1)}{\partial n} & \frac{\partial u_n^*(x_1 - y_2)}{\partial n} & \cdots & \frac{\partial u_n^*(x_1 - y_N)}{\partial n} \\ \frac{\partial u_n^*(x_2 - y_1)}{\partial n} & \frac{\partial u_n^*(x_2 - y_2)}{\partial n} & \cdots & \frac{\partial u_n^*(x_2 - y_N)}{\partial n} \\ \vdots & \vdots & \ddots & \vdots \\ \frac{\partial u_n^*(x_N - y_1)}{\partial n} & \frac{\partial u_n^*(x_N - y_2)}{\partial n} & \cdots & \frac{\partial u_n^*(x_N - y_N)}{\partial n} \end{pmatrix}. \tag{3.4}$$

It is easy to prove that the matrix A in (3.3) is circulant, defined by

$$A = \text{circ}(u_n^*(x_1 - y_1), u_n^*(x_1 - y_2), \dots, u_n^*(x_1 - y_N)). \tag{3.5}$$

By some basic algebraic operation, we have

$$\frac{\partial u_n^*(x_i - y_j)}{\partial n} = \frac{\partial u_n^*(x_i - y_j)}{\partial r} (1 - s \cos(\psi_i - \psi_j)). \tag{3.6}$$

The matrix equation (3.4) is also circulant given by

$$A = \text{circ}\left(\frac{\partial u_n^*(x_1 - y_1)}{\partial n}, \frac{\partial u_n^*(x_1 - y_2)}{\partial n}, \dots, \frac{\partial u_n^*(x_1 - y_N)}{\partial n}\right). \tag{3.7}$$

For three dimensional problems, we do have the matrix with circulant submatrix. Taking the ellipsoid solution domain as an example, the collocation points $x_{mi} = \{x_{mi}, y_{mi}, z_{mi}\}_{m=1, i=1}^{M, N}$ on Γ are taken to be

$$x_{mi} = \{r_a \sin(\psi_m) \cos(\phi_i), r_b \sin(\psi_m) \sin(\phi_i), r_c \cos(\psi_m)\}, \tag{3.8}$$

where

$$\psi_m = \frac{\pi m}{M+1}, \quad \phi_i = \frac{2\pi(i-1)}{N}, \quad m = 1, 2, \dots, M, \quad i = 1, 2, \dots, N. \tag{3.9}$$

Similarly, the singularities can be chosen as follows

$$y_{nj} = \{sr_a \sin(\psi_n) \cos(\phi_j), sr_b \sin(\psi_n) \sin(\phi_j), sr_c \cos(\psi_n)\}, \tag{3.10}$$

where $0 < s < 1$. Then (2.6) yields the following matrix equation

$$A\beta = f, \tag{3.11}$$

where the $MN \times MN$ matrix A has the structure

$$A = \begin{pmatrix} A_{11} & A_{12} & \cdots & A_{1M} \\ A_{21} & A_{22} & \cdots & A_{2M} \\ \vdots & \vdots & \ddots & \vdots \\ A_{M1} & A_{M2} & \cdots & A_{MM} \end{pmatrix}, \tag{3.12}$$

in which

$$A_{kl} = \begin{pmatrix} u_n^*(x_{k1} - y_{l1}) & u_n^*(x_{k1} - y_{l2}) & \cdots & u_n^*(x_{k1} - y_{lN}) \\ u_n^*(x_{k2} - y_{l1}) & u_n^*(x_{k2} - y_{l2}) & \cdots & u_n^*(x_{k2} - y_{lN}) \\ \vdots & \vdots & \ddots & \vdots \\ u_n^*(x_{kN} - y_{l1}) & u_n^*(x_{kN} - y_{l2}) & \cdots & u_n^*(x_{kN} - y_{lN}) \end{pmatrix}, \tag{3.13}$$

or

$$A_{kl} = \begin{pmatrix} \frac{\partial u_n^*(x_{k1}-y_{l1})}{\partial n} & \frac{\partial u_n^*(x_{k1}-y_{l2})}{\partial n} & \dots & \frac{\partial u_n^*(x_{k1}-y_{lN})}{\partial n} \\ \frac{\partial u_n^*(x_{k2}-y_{l1})}{\partial n} & \frac{\partial u_n^*(x_{k2}-y_{l2})}{\partial n} & \dots & \frac{\partial u_n^*(x_{k2}-y_{lN})}{\partial n} \\ \vdots & \vdots & \ddots & \vdots \\ \frac{\partial u_n^*(x_{kN}-y_{l1})}{\partial n} & \frac{\partial u_n^*(x_{kN}-y_{l2})}{\partial n} & \dots & \frac{\partial u_n^*(x_{kN}-y_{lN})}{\partial n} \end{pmatrix}. \tag{3.14}$$

It is clear that the submatrix A_{kl} in (3.13) is circulant. We also note that (3.14) also has circulant feature which can be proved as follows,

$$\begin{aligned} \frac{\partial u_n^*(x_{ki}-y_{lj})}{\partial n} &= \frac{\partial u_n^*(x_{ki}-y_{lj})}{\partial r} \frac{\partial r}{\partial n} = \frac{\partial u_n^*(x_{ki}-y_{lj})}{\partial r} \frac{\Delta xn_1 + \Delta yn_2 + \Delta zn_3}{r} \\ &= \frac{\partial u_n^*(x_{ki}-y_{lj})}{\partial r} \frac{(2 - 2s\cos(\psi_k)\cos(\psi_l) - 2s\sin(\psi_k)\sin(\psi_l)\cos(\phi_i - \phi_j))}{(Lr)}, \end{aligned} \tag{3.15}$$

where L is given by

$$L = \sqrt{\frac{4\sin^2(\psi_k)}{r_a^2} + \frac{4\cos^2(\psi_k)}{r_c^2}},$$

since $r_a = r_b$ for ellipsoid domain. Here we have proved that matrices (3.3) and (3.12) have the structure of circulant matrix which can be solved efficiently. Without loss of generality, we consider the following $N \times N$ circulant matrix

$$C = \text{circ}(c_1, c_2, \dots, c_N). \tag{3.16}$$

It is known that the circulant matrix can be factored into the product of the the following matrices [9]

$$C = U^*DU, \tag{3.17}$$

where

$$U^* = \frac{1}{N^{1/2}} \begin{pmatrix} 1 & 1 & 1 & \dots & 1 \\ 1 & w & w^2 & \dots & w^{N-1} \\ 1 & w^2 & w^4 & \dots & w^{2(N-1)} \\ \vdots & \vdots & \vdots & \ddots & \vdots \\ 1 & w^{N-1} & w^{2(N-1)} & \dots & w^{(N-1)(N-1)} \end{pmatrix}, \tag{3.18}$$

and

$$D = \text{diag}(d_1, d_2, \dots, d_N), \quad d_i = \sum_{k=1}^N c_k w^{(k-1)(i-1)}, \tag{3.19}$$

with $w = e^{2\pi i/N}$.

We denote \otimes as the matrix tensor product. Note that [9]

$$(I_M \otimes U^*)(I_M \otimes U) = I_{MN}. \tag{3.20}$$

From (3.11), multiplying both sides by the block diagonal matrix $I_M \otimes U$ yields

$$(I_M \otimes U)A(I_M \otimes U^*)(I_M \otimes U)\beta = (I_M \otimes U)f. \tag{3.21}$$

The above equation can be written as follows

$$\bar{A}\bar{\beta} = \bar{f}, \tag{3.22}$$

where

$$\begin{aligned} \bar{A} &= (I_M \otimes U)A(I_M \otimes U^*) = \begin{pmatrix} UA_{11}U^* & UA_{12}U^* & \cdots & UA_{1M}U^* \\ UA_{21}U^* & UA_{22}U^* & \cdots & UA_{2M}U^* \\ \vdots & \vdots & \ddots & \vdots \\ UA_{M1}U^* & UA_{M2}U^* & \cdots & UA_{MM}U^* \end{pmatrix} \\ &= \begin{pmatrix} D_{11} & D_{12} & \cdots & D_{1M} \\ D_{21} & D_{22} & \cdots & D_{2M} \\ \vdots & \vdots & \ddots & \vdots \\ D_{M1} & D_{M2} & \cdots & D_{MM} \end{pmatrix}, \end{aligned} \tag{3.23a}$$

$$\bar{\beta} = (I_M \otimes U)\beta, \tag{3.23b}$$

and

$$\bar{f} = (I_M \otimes U)f. \tag{3.24}$$

Note that each of the $N \times N$ block matrix D_{kl} in (3.23) is diagonal. In particular, if the submatrix of A

$$A_{ij} = \text{circ}(c_1, c_2, \dots, c_N) = \begin{pmatrix} c_1 & c_2 & \cdots & c_N \\ c_N & c_1 & \cdots & c_{N-1} \\ \vdots & \vdots & \ddots & \vdots \\ c_2 & c_3 & \cdots & c_1 \end{pmatrix}, \tag{3.25}$$

then the corresponding submatrix $D_{ij} = \text{diag}(d_{ij}^1, d_{ij}^2, \dots, d_{ij}^N)$, where

$$d_{ij}^l = \sum_{k=1}^N c_k w^{(k-1)(l-1)}, \quad l = 1, 2, \dots, N. \tag{3.26}$$

Since the matrix equation (3.11) has been decomposed into M^2 blocks of the rank N each of which is diagonal, the solution to (3.11) can be decomposed into N systems of equations with rank M ,

$$E_l \beta_l = (\bar{f}_l), \quad l = 1, 2, \dots, N, \tag{3.27}$$

where

$$(E_l)_{ij} = d_{ij}^l, \quad i, j = 1, 2, \dots, M, \quad l = 1, 2, \dots, N, \tag{3.28a}$$

$$(\bar{f}_l)_i = (\bar{f})_{(i-1)N+l}, \quad i = 1, 2, \dots, M, \quad l = 1, 2, \dots, N. \tag{3.28b}$$

In conclusion, we have the following algorithm:

Step 1 Compute $\bar{f} = (I_M \otimes U)f$,

Step 2 Construct the diagonal matrix D_{ij} in (3.23),

Step 3 Solve N linear system of equations of order M to obtain the $\bar{\beta}$ in (3.23b),

Step 4 Recover the β from (3.23b).

It is noted that in Steps 1, 2 and 4, fast Fourier transform and inverse fast Fourier transform can be used to save the memory space and speed up the computation while the most expensive part of the algorithm is to solve N complex linear systems of order M which can be done by Gaussian elimination at a cost of $\mathcal{O}(NM^3)$.

4 Numerical results and discussions

To demonstrate the efficiency of the algorithm proposed in this paper, several numerical examples are investigated. The L_2 relative average error to be shown in this section is defined as:

$$\text{Error} = \sqrt{\frac{\sum_{j=1}^{N_t} (u(x_j, y_j) - \tilde{u}(x_j, y_j))^2}{\sum_{j=1}^{N_t} (u(x_j, y_j))^2}},$$

where (x_j, y_j) denotes the j -th test point, N_t is the total number of randomly distributed test points for both two and three dimensional problems, u and \tilde{u} are the exact and numerical solution respectively.

It is noted that the computation were carried out on MATLAB^{2011b} platform in OS Windows 7 (64bit) with I3 3.30GHz CPU and 16GB memory. For all the examples in this section, k denotes the wave-number, s the ratio between the fictitious boundary and physical boundary, sr the radius of fictitious circular or spherical boundary, N the number of collocation points. The number of source points is taken to be the same as the number of collocation points. In this section, we choose $N_t = 100$ for all the examples.

4.1 Two-dimensional cylinder radiation model under Neumann boundary condition

In this example, we consider the radiation problem of an infinite circular cylinder with Neumann boundary condition as shown in Fig. 1. The analytical solution u of the radiation field is given by

$$u(r, \theta) = -\frac{kaH_4^{(1)}(kr)}{kaH_3^{(1)}(ka) - 4H_4^{(1)}(ka)} \cos(4\theta), \quad (4.1)$$

where $H_m^{(1)}$ is a Hankel function of the first kind of order m , and a is the radius of the cylinder and the corresponding Neumann boundary condition is given by

$$\frac{\partial u}{\partial n} = k \cos(4\theta). \quad (4.2)$$

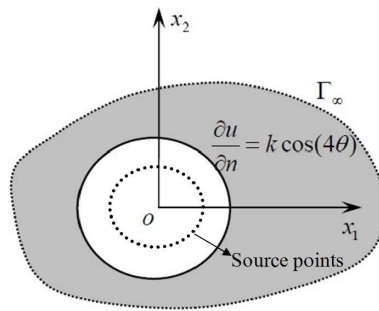


Figure 1: The profile of the physical domain of an infinite cylinder.

In particular, we consider the cylinder with radius $a = 100$. In Fig. 2, we present the L_2 errors versus the radius of fictitious boundary in the case of wave-number $k = 100$ with different number of collocation points $N = 100, 1,000, 10,000$ and $20,000$. From this figure, we can see that when N is small, the radius of fictitious boundary is critical to the accuracy of the MFS approximation. When N becomes larger, more accurate and stable results can be achieved disregard to the radius of fictitious boundary sr . This indicates that we can use more collocation points to alleviate the uncertainty of choosing the fictitious boundary which is a difficult issue for the traditional MFS.

To show the efficiency of the MFS in the context of wave-number k , we display errors versus N using $sr = 80$ as shown in Fig. 3. We observe that the MFS performs very well

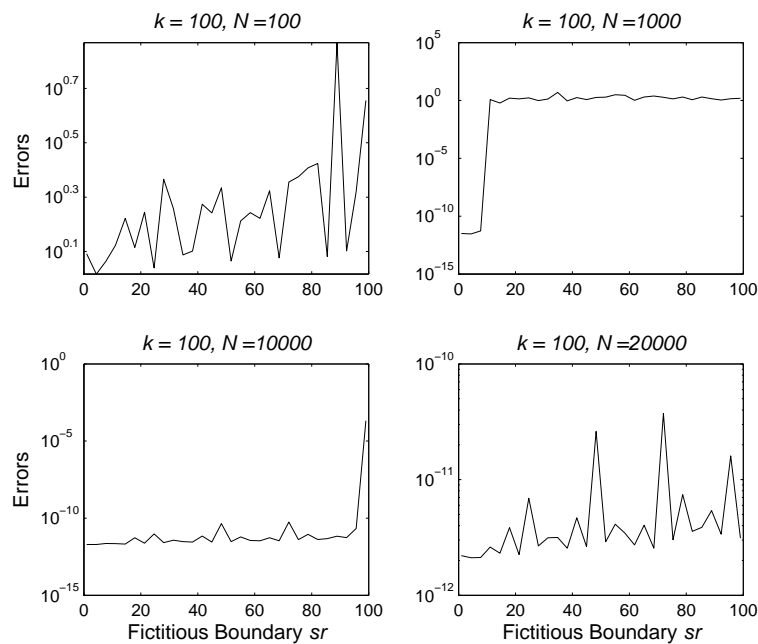


Figure 2: Errors versus of the radius of the fictitious boundary with different number of collocation points in the case of $k = 100$.

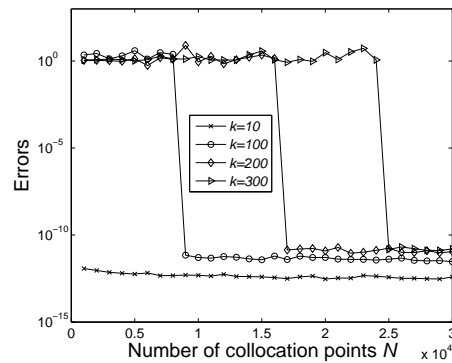


Figure 3: Errors versus the number of collocation points with different wave-number k in the case of $sr=80$.

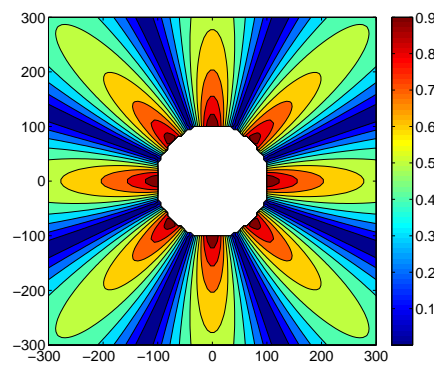


Figure 4: The profile of numerical solution with $k=300$ and $sr=80$.

with the increasing number of collocation points. For larger wave-number k , we should use more collocation points to obtain acceptable results. The profile of numerical solution for wave-number $k=300$ is shown in Fig. 4.

To show the capability of the fast MFS algorithm for handling much large wave-number k , we display the numerical errors versus N with wave-number $k=10,000$ and $sr=80$ in Fig. 5. We observe that the MFS converges very well and numerical accuracy reaches 10^{-10} for $N \geq 3 \times 10^6$. In Fig. 5, we note that the computational time increases linearly proportional to N when $N < 8 \times 10^7$; i.e., $\mathcal{O}(N)$. Even for $N=10^8$, we can obtain the numerical solution roughly in 100 seconds which is unthinkable in contrast to the traditional approach of the MFS.

4.2 Three-dimensional ellipsoid radiation model under Dirichlet boundary condition

In this case, we consider the scattering problems on an exterior ellipsoid domain

$$\Omega_+ = \left\{ (x, y, z) \mid \left(\frac{x}{a}\right)^2 + \left(\frac{y}{b}\right)^2 + \left(\frac{z}{c}\right)^2 \geq 1 \right\}$$

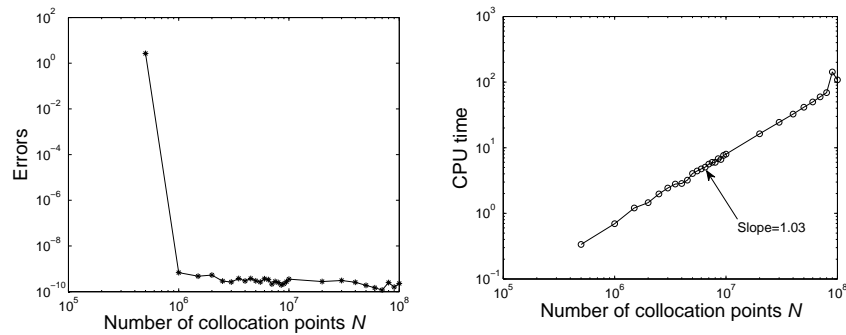


Figure 5: Errors (left) and CPU time (right) versus the number of collocation points with $k=10,000$ and $sr=80$.

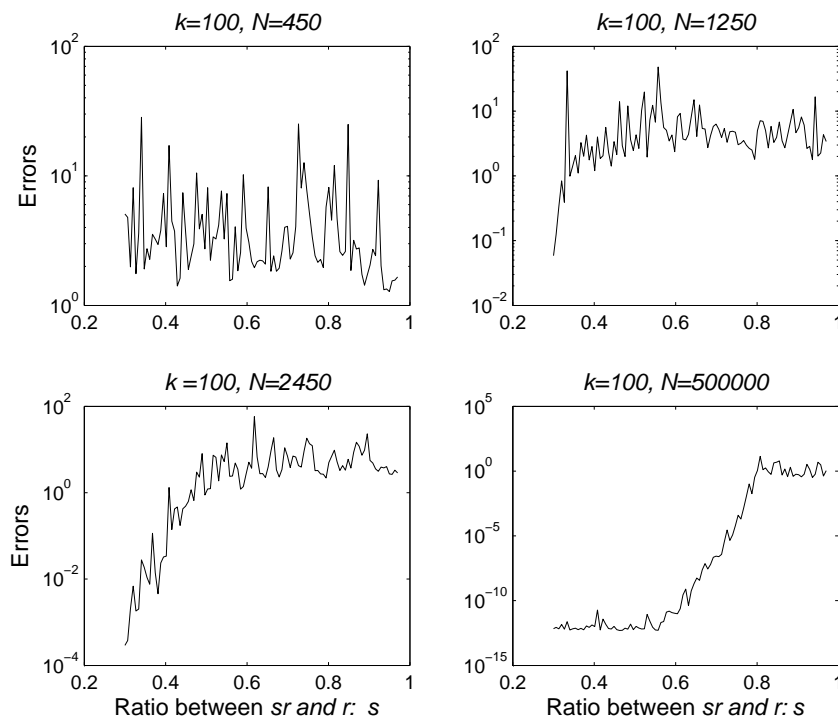


Figure 6: Results for varying parameter s and various collocation points N in the case of ellipsoid domain with $k=100$.

with Dirichlet boundary condition

$$u(x,y,z) = \frac{e^{ikR_0}}{R_0}, \quad (x,y,z) \in \partial\Omega_+, \tag{4.3}$$

where $R_0 = \sqrt{x^2 + y^2 + z^2}$. The analytical solution is given by

$$u(x,y,z) = \frac{e^{ikr}}{r}, \quad (x,y,z) \in \Omega_+, \tag{4.4}$$

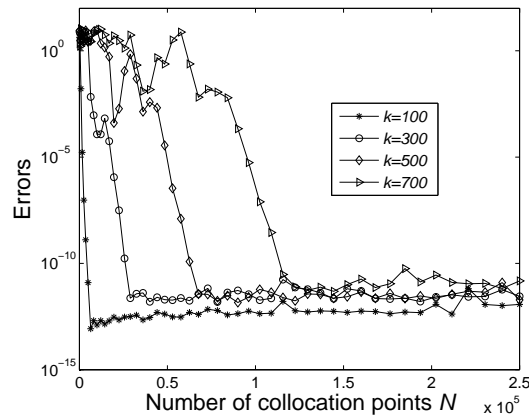


Figure 7: Errors versus of the number of collocation points with different wave-number k with $s=0.3$.

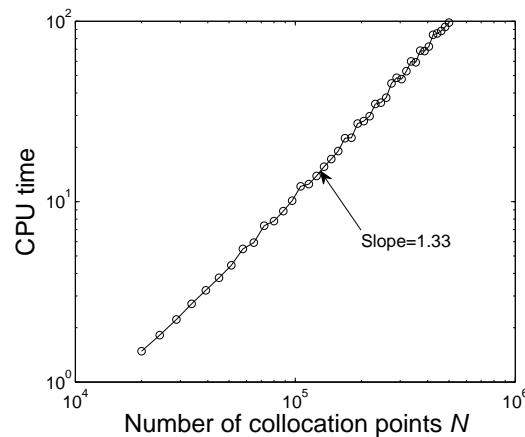


Figure 8: CPU time versus the number of collocation points with $k=600$ and $s=0.3$.

where $r = \sqrt{x^2 + y^2 + z^2}$. In this example, the parameters of the ellipsoid are chosen as $a=b=0.8$, $c=1$.

In Fig. 6, we present the L_2 errors versus the ratio between the fictitious boundary and physical boundary with different number of collocation points $N = 450, 1,250, 2,450$ and $500,000$. As before, the fictitious boundary is critical to the numerical accuracy. With more collocation points, we can obtain more accurate results. The numerical results reveal that for large N , errors becomes less dependent on sr which can be verified from the bottom right figure in Fig. 6.

Convergent study is displayed in Fig. 7. From which we can observe that the MFS approximation converges very well with respect to N . For high wave-number k , we need much more collocation points to maintain the same accuracy just as mentioned in the previous examples. Finally, we show the CPU time versus N in Fig. 8 with $k=600$ and $s=0.3$. Note that the CPU time increases superlinearly with respect to N ; i.e., $\mathcal{O}(N^{1.33})$.

4.3 Three-dimensional pulsating-sphere model under Neumann boundary condition

Finally, we consider the acoustic radiation from a pulsating sphere as shown in Fig. 9. This sphere is applied with uniform radial velocity v_0 . Therefore, the corresponding analytical solution of the pulsating-sphere problem can be derived as follows [30]

$$u(r, \theta_1, \theta_2) = \frac{a}{r} \left(\frac{ikaz_0}{ika-1} \right) v_0 e^{ik(r-a)}, \quad (4.5)$$

where a is the radius of the sphere and $z_0 = \rho_0 c_0$ is the characteristic impedance of the medium in which ρ_0 represents the density of the medium and c_0 is the sound velocity. This example is often used as a benchmark problem to verify the algorithm. In this example, we choose $a = 1$.

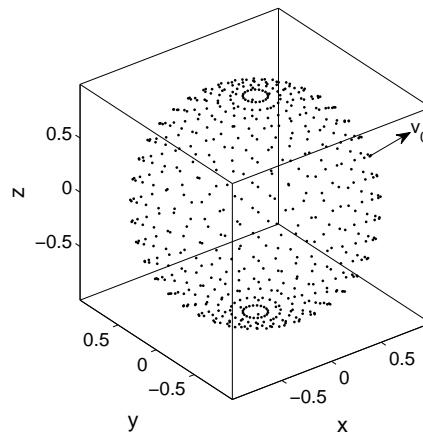


Figure 9: Sketch of the pulsating model with uniform radial velocity v_0 .

In Fig. 10, we display the errors of $|u/(v_0 z_0)|$ versus the fictitious boundary with various number of collocation points. From the figure we come to the same conclusion as in the previous two examples that the larger N will have positive impact on the location of fictitious boundary. Convergent results are shown in Figs. 10 and 11. We observe that the MFS converges very well along the increase of the number of collocation points. For the high wave-number k , more collocation points should be used. Finally we show the CPU time versus N for $k=1,000$ and $sr=0.3$ in Fig. 12. We can obtain the numerical solution in 120 seconds with $N=500,000$. The CPU time increases superlinearly with respect to N ; i.e., $\mathcal{O}(N^{1.52})$.

5 Concluding remarks

In this paper, the MFS is used to solve high wave-number exterior Helmholtz problems in the axisymmetric domain. Due to the symmetric property of the circulant matrix, a ma-

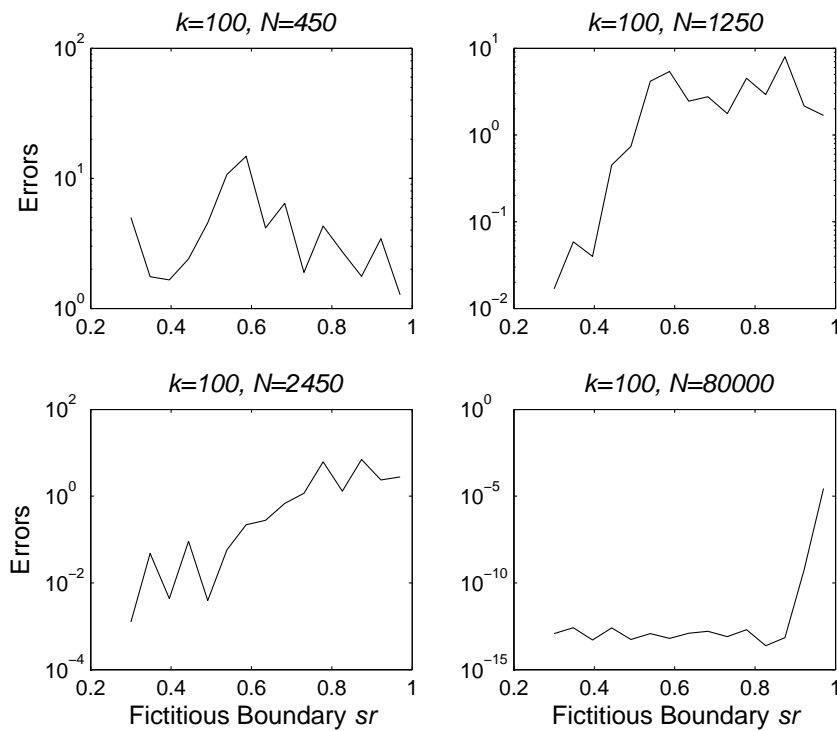


Figure 10: Errors versus of the radius of the fictitious boundary with different number of collocation points in the case of $k=100$ for example 3.

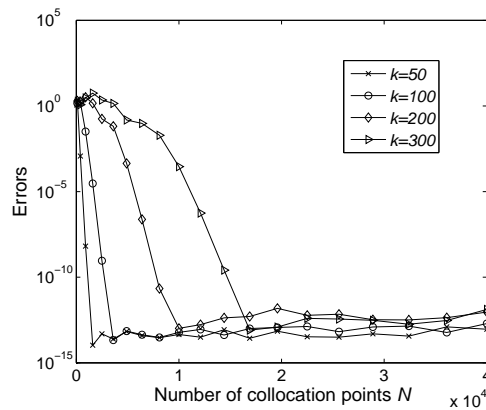


Figure 11: Convergence study for different wave-number k with $sr=0.3$.

trix decomposition algorithm is implemented to accelerate the solution process. Three numerical examples demonstrate the efficiency of MFS for solving large wave-number Helmholtz problems. We observe that the CPU time increases linearly for two dimensional problems and superlinearly for three dimensional problems. Hence, even with a large number of collocation points being used, the computational time is still very reason-

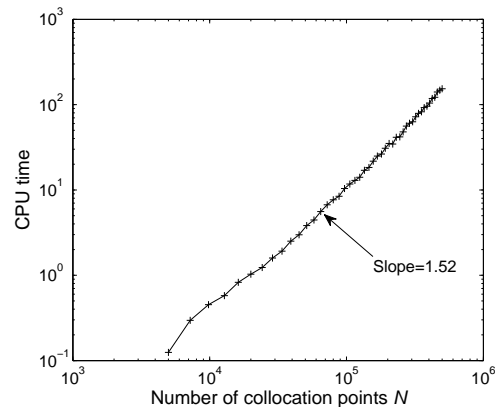


Figure 12: CPU time versus the number of collocation points with $k=1,000$ and $sr=0.3$.

able. One of the restrictions of our proposed approach is that the computational domain has to be axisymmetric. For the irregular domain, a conformal mapping can be considered to transform the given domain to a circular domain [15]. This will be the subject of our future investigation.

Acknowledgments

The work described in this paper was supported by National Basic Research Program of China (973 Project No. 2010CB832702), the R&D Special Fund for Public Welfare Industry (Hydrodynamics, Project No. 201101014 and the 111 project under grant B12032), National Science Funds for Distinguished Young Scholars (Grant No. 11125208). The third author acknowledges the support of Distinguished Overseas Visiting Scholar Fellowship provided by the Ministry of Education of China.

References

- [1] CARLOS J. S. ALVES, M. A. VITOR AND LEITÃO, *Crack analysis using an enriched MFS domain decomposition technique*, Eng. Anal. Bound. Elem., 30 (2006), pp. 160–166.
- [2] CARLOS J. S. ALVES AND SVILEN S. VALTCHEV, *Numerical comparison of two meshfree methods for acoustic wave scattering*, Eng. Anal. Bound. Elem., 29 (2005), pp. 371–382.
- [3] C. A. BREBBIA AND L. C. WROBEL, *The boundary element method*, Comput. Methods Fluid, London, Pentech Press, Ltd., 1980, pp. 26–48.
- [4] B. BIN-MOHSIN AND D. LESNIC, *Determination of inner boundaries in modified Helmholtz inverse geometric problems using the method of fundamental solutions*, Math. Comput. Simulation, 82 (2012), pp. 1445–1458.
- [5] A. BAYLISS AND E. TURKE, *Radiation boundary conditions for wave-like equations*, Commun. Pure Appl. Math., 33 (2006), pp. 707–725.

- [6] A. H. BARNETT AND T. BETCKE, *Stability and convergence of the method of fundamental solutions for Helmholtz problems on analytic domains*, J. Comput. Phys., 227 (2008), pp. 7003–7026.
- [7] C. S. CHEN, H. A. CHO AND M. A. GOLBERG, *Comments on the ill-conditioning of the method of fundamental solutions*, Eng. Anal. Bound. Elem., 30 (2009), pp. 405–410.
- [8] T. W. DROMBOSKY, A. L. MEYER AND L. LING, *Applicability of the method of fundamental solutions*, Eng. Anal. Bound. Elem., 33 (2009), pp. 637–643.
- [9] P. J. DAVIS, *Circulant Matrices*, John Wiley & Sons, New York, Chichester, Brisbane, 1979.
- [10] G. FAIRWEATHER, A. KARAGEORGHIS AND Y. S. SMYRLIS, *A matrix decomposition MFS algorithm for axisymmetric biharmonic problems*, Adv. Comput. Math., 23 (2005), pp. 55–71.
- [11] G. FAIRWEATHER AND A. KARAGEORGHIS, *The method of fundamental solutions for elliptic boundary value problems*, Adv. Comput. Math., 9 (1998), pp. 69–95.
- [12] G. FAIRWEATHER, A. KARAGEORGHIS AND P. A. MARTIN, *The method of fundamental solutions for scattering and radiation problems*, Eng. Anal. Bound. Elem., 27 (2003), pp. 759–769.
- [13] M. A. GOLBERG, *The method of fundamental solutions for Poisson's equation*, Eng. Anal. Bound. Elem., 16 (1995), pp. 205–213.
- [14] M. A. GOLBERG AND C. S. CHEN, *The method of fundamental solutions for potential, Helmholtz and diffusion problems*, in: M. A. Golberg (Eds.), *Boundary integral methods-numerical and mathematical aspects*, Computational Mechanics Publications, 1998, pp.103–176.
- [15] A. R. H. HERYUDONO AND T. A. DRISCOLL, *Radial basis function interpolation on irregular domain through conformal transplanation*, J. Sci. Comput., 44 (2010), pp.286–300.
- [16] Y. C. HON AND T. WEI, *A fundamental solution method for inverse heat conduction problem*, Eng. Anal. Bound. Elem., 28 (2004), pp. 489–495.
- [17] A. KARAGEORGHIS, C. S. CHEN AND Y. S. SMYRLIS, *Matrix decomposition RBF algorithm for solving 3D elliptic problems*, Eng. Anal. Bound. Elem., 33 (2009), pp. 1368–1373.
- [18] A. KARAGEORGHIS AND Y. S. SMYRLIS, *Conformal mapping for the efficient MFS solution of Dirichlet boundary value problems*, Computing, 83 (2008), pp. 1–24.
- [19] A. KARAGEORGHIS AND G. FAIRWEATHER, *The method of fundamental solutions for axisymmetric potential problems*, Int. J. Numer. Methods Eng., 44 (1999), pp. 1653–1669.
- [20] A. KARAGEORGHIS AND G. FAIRWEATHER, *The method of fundamental solutions for axisymmetric elasticity problems*, Comput. Mech., 25 (2000), pp. 524–532.
- [21] A. KARAGEORGHIS AND G. FAIRWEATHER, *The method of fundamental solutions for axisymmetric acoustic scattering and radiation problems*, J. Acoustic Soc. Am., 104 (1998), pp. 3212–3218.
- [22] T. KITAGAWA, *On the numerical stability of the method of fundamental solution applied to the Dirichlet problem*, Japan J. Industrial Appl. Math., 5 (1988), pp. 123–133.
- [23] X. L. LI AND J. L. ZHU, *The method of fundamental solutions for nonlinear elliptic problems*, Eng. Anal. Bound. Elem., 33 (2009), pp. 322–329.
- [24] J. C. LI AND Y. C. HON, *Domain decomposition for radial basis meshless methods*, Numer. Methods Partial Differential Equations, 20 (2004), pp. 450–462.
- [25] N. S. MERA, *The method of fundamental solutions for the backward heat conduction problem*, Inverse Prob. Sci. Eng., 13 (2005), pp. 65–78.
- [26] A. NEUMAIER, *Solving ill-conditioned and singular linear systems: a tutorial on regularization*, SIAM Rev., 40 (1998), pp. 636–666.
- [27] P. A. RAMACHANDRAN, *Method of fundamental solutions: singular value decomposition analysis*, Commun. Numer. Methods Eng., 18 (2002), pp. 789–801.
- [28] Y. S. SMYRLIS AND A. KARAGEORGHIS, *Some aspects of the method of fundamental solutions for certain harmonic problems*, J. Sci. Comput., 16 (2001), pp. 341–371.
- [29] Y. S. SMYRLIS AND A. KARAGEORGHIS, *Some aspects of the method of fundamental solutions for*

- certain biharmonic problems*, Comput. Model. Eng. Sci., 4 (2003), pp. 535–550.
- [30] A. F. SEYBERT, B. SOENARKO, F. J. RIZZO AND D. J. SHIPPY, *An advanced computational method for radiation and scattering of acoustic waves in three dimensions*, The Journal of Acoustical Society of America, 77 (1985), pp. 362–368.
- [31] TH. TSANGARIS, Y. S. SMYRLIS AND A. KARAGEORGHIS, *A matrix decomposition mfs algorithm for problems in hollow axisymmetric domains*, J. Sci. Comput., 28 (2006), pp. 31–50.
- [32] T. WEI, Y. C. HON AND L. LING, *Method of fundamental solutions with regularization techniques for Cauchy problems of elliptic operators*, Eng. Anal. Bound. Elem., 31 (2007), pp. 373–385.
- [33] D. L. YOUNG, C. C. TSAI, C. W. CHEN AND C. M. FAN, *The method of fundamental solutions and condition number analysis for inverse problems of Laplace equations*, Comput. Math. Appl., 55 (2008), pp. 1189–1200.
- [34] D. L. YOUNG, C. M. FAN, C. C. TSAI AND C. W. CHEN, *The method of fundamental solutions and domain decomposition method for degenerate seepage flownet problems*, Journal of the Chinese Institute of Engineering, 20 (2006), pp. 63–73.
- [35] O. C. ZIENKIEWICZ, D. W. KELLY AND P. BETTESS, *The sommerfeld (radiation) condition on infinite domains and its modelling in numerical procedures*, Comput. Methods Appl. Sci. Eng., 704 (1979), pp. 169–203.